C201 Viscous Flow and Turbulence

Lecture 3

Part 2: More linear eddy viscosity models

Luca di Mare

St John's College

1 The $k-\varepsilon$ Model

The original $k-\varepsilon$ model was published by W.P. Jones (your lecturer's PhD supervisor) and B.E. Launder (Jones' own MSc and then PhD supervisor) at Imperial College London (back then Imperial College of Science, Medicine and Technology). The original publication is:

W.P. Jones, B.E. Launder, The prediction of laminarization with a two-equation model of turbulence, International Journal of Heat and Mass Transfer, Volume 15, Issue 2, 1972,Pages 301-314

The model was formulated to address the relaminarization process in accelerating boundary layers. This problem requires a realistic estimate of the rise of the dissipation rate ε in presence of streamwise acceleration. The model solves two coupled transport equations, one for k and the other for $\varepsilon = \nu \overline{\frac{\partial u_i'}{\partial x_j}\frac{\partial u_i'}{\partial x_j}}$. The model infers u' from k and ℓ_{Mix} from ε. The relation between ν_T and the model variables is:

$$\nu_T = C_\mu k^2/\varepsilon$$

where C_μ is an empirical constant. Comparison with the mixing length model shows that

$$\nu \approx \ell u' \rightarrow \ell \approx \frac{k^{\frac{3}{2}}}{\varepsilon}$$

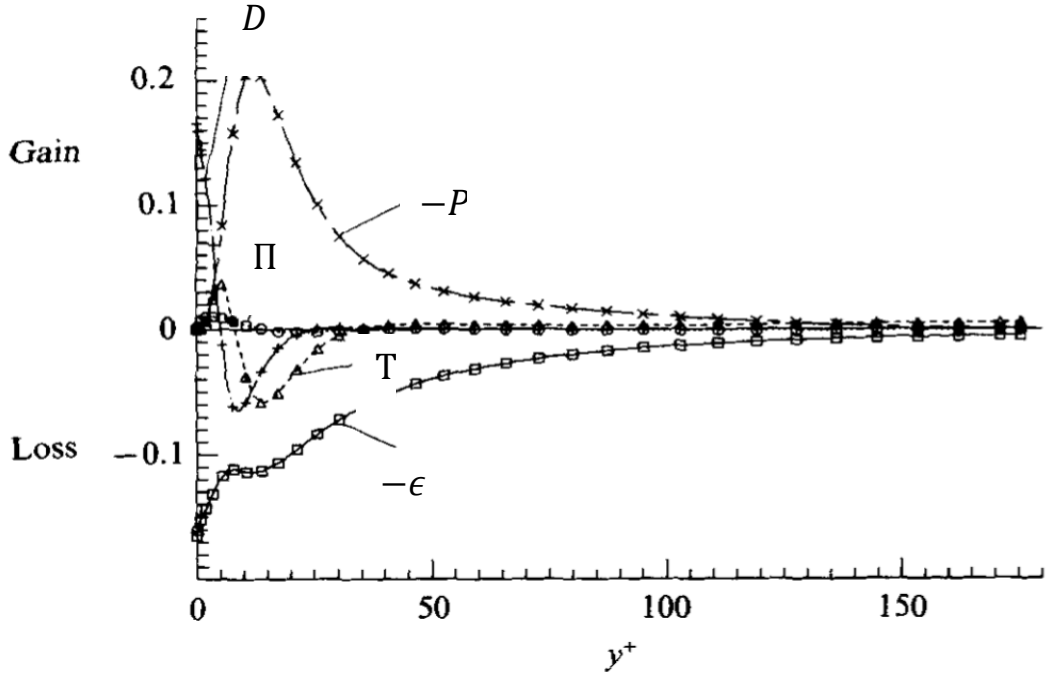

Figure 1: TKE budget in turbulent channel flow at $Re_\tau = 180$, from Mansour, N., Kim, J., & Moin, P. (1988). Reynolds-stress and dissipation-rate budgets in a turbulent channel flow. *Journal of Fluid Mechanics, 194*, 15-44.

The transport equations of the model are

$$\frac{\partial k}{\partial t} + U_j \frac{\partial k}{\partial x_j} = \tau_{ij} \frac{\partial U_i}{\partial x_j} - \varepsilon + \frac{\partial}{\partial x_j}\left(\left(\nu + \frac{\nu_T}{\sigma_k}\right)\frac{\partial k}{\partial x_j}\right)$$

$$\frac{\partial \varepsilon}{\partial t} + U_j \frac{\partial \varepsilon}{\partial x_j} = C_{\varepsilon 1} \frac{\varepsilon}{k} \tau_{ij} \frac{\partial U_i}{\partial x_j} - C_{\varepsilon 2} \frac{\varepsilon^2}{k} + \frac{\partial}{\partial x_j}\left(\left(\nu + \frac{\nu_T}{\sigma_\varepsilon}\right)\frac{\partial \varepsilon}{\partial x_j}\right)$$

For comparison, the “exact” TKE equation derived earlier in the module

$$U_j \frac{\partial k}{\partial x_j} = \tau_{ij} \frac{\partial U_i}{\partial x_j} - \varepsilon + \nu \frac{\partial^2 k}{\partial x_j \partial x_j} - \frac{1}{\rho} \overline{u_\iota' \frac{\partial p'}{\partial x_\iota}} - \frac{\partial}{\partial x_j} \overline{u_j' u_\iota' u_\iota'}$$

It can be seen that the exact TKE equation and the $k - \varepsilon$ equation differ because the velocity-pressure correlation and the triple correlation are lumped in a modelled turbulent diffusion term, but are otherwise very similar. Also, the DNS TKE budget for turbulent channel flow shows that the velocity pressure gradient term is in fact small.

The equation for ε, on the other hand, differs considerably from the exact transport equation for the dissipation rate (see Mansour et al for the ε transport equation). The main difficulty here is twofold. Firstly, many of the terms in the exact ε transport equation cannot be easily inferred from the mean flow. Secondly, ε is determined by the smallest eddies, which are inaccessible to the RANS solution.

ε is essentially used to determine the mixing length, which is influenced by the integral scales, because it is the largest eddies that contribute most to the Reynolds stress. There is therefore an intrinsic ambiguity in the meaning of the ε variable of the $k-\varepsilon$ model: it is representative of the smallest scales of motion, but is used to extract information about the mixing length, which is closer to the integral scale.

Closure coefficients and relations:

$$C_{\varepsilon 1} = 1.44, \quad C_{\varepsilon 2} = 1.92, \quad C_{\varepsilon \mu} = 0.09, \qquad \sigma_k = 1.0, \quad \sigma_\varepsilon = 1.3$$

$$\omega = \varepsilon/(C_\mu k), \qquad l = C_\mu k^{3/2}/\varepsilon$$

The $k-\varepsilon$ model has grown into an extensive family models. Members of this family feature, among other modifications:

- Modified coefficients
- Mean velocity gradients (e.g. "*realisable*" *k*-ε models).
- Others have a different ε equation.

1.1 Chien's low-Reynolds number corrections

The $k-\varepsilon$ model with closure coefficients in the previous section is not suitable to operate in close proximity of solid walls because it tries to return finite values of eddy viscosity and Reynolds stress at solid walls which are unphysical. There are several ways of correcting this behaviour. Most published contributions modify the model by introducing five auxiliary functions, f_μ, f_1, f_2,e_0, e_1 with the purpose of turning off the eddy viscosity and the production terms near solid walls (f_μ, f_1, f_2) while at the same time introducing extra dissipation to reduce the values of both k and ε towards 0.

$$\frac{\partial k}{\partial t} + U_j \frac{\partial k}{\partial x_j} = \tau_{ij} \frac{\partial U_i}{\partial x_j} - \varepsilon - e_0 + \frac{\partial}{\partial x_j}\left(\left(\nu + \frac{\nu_T}{\sigma_k}\right)\frac{\partial k}{\partial x_j}\right)$$

$$\frac{\partial \varepsilon}{\partial t} + U_j \frac{\partial \varepsilon}{\partial x_j} = f_1 C_{\varepsilon 1} \frac{\varepsilon}{k} \tau_{ij} \frac{\partial U_i}{\partial x_j} - f_2 C_{\varepsilon 2} \frac{\varepsilon^2}{k} + e_1 + \frac{\partial}{\partial x_j}\left(\left(\nu + \frac{\nu_T}{\sigma_\varepsilon}\right)\frac{\partial \varepsilon}{\partial x_j}\right)$$

$$\nu_T = f_\mu C_\mu k^2/\varepsilon$$

One contribution is Chien's model which is defined by the following auxiliary relations:

$$Re_T = \frac{k^2}{\varepsilon \nu}$$

$$f_\mu = 1 - e^{-0.0015\, y^+}$$

$$f_1 = 1$$

$$f_2 = 1 - 0.22 e^{-\frac{Re_T^2}{36}}$$

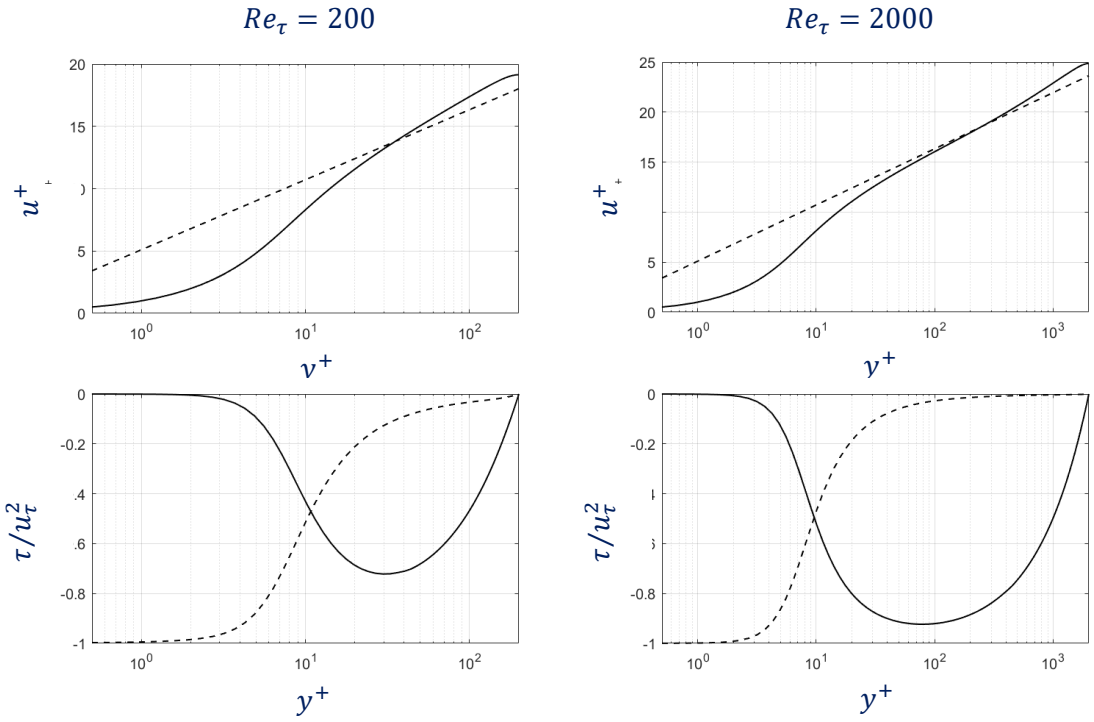

Figure 2: mean velocity profile and stress distributions from Chien's $k-\varepsilon$ model for turbulent channel flow at Re_τ 200 and 2000

$$e_0 = \frac{2\nu k}{y^2}$$

$$e_1 = -\frac{2\nu\varepsilon}{y^2} e^{-y^+/2}$$

where y is the distance from the wall and the model constants are also modified:

$$C_{\varepsilon 1} = 1.45, \quad C_{\varepsilon 2} = 1.8, \quad C_{\varepsilon\mu} = 0.09, \quad \sigma_k = 1.0, \quad \sigma_\varepsilon = 1.3$$

The boundary conditions for the k and ε variables of the various $k-\varepsilon$ models are not always straightforward. For Chien's model the correct boundary conditions at a wall are

$$k \to 0$$

$$\varepsilon \to 0$$

1.2 Turbulent channel flow with Chien's model

Mean velocity profiles and stresses from Chien's model are show in Figure 2. The model generates profiles that follow the log-law closely at both Reynolds numbers. At the higher Reynolds number the agreement with the logarithmic law of the wall is closer.

The k variable in Chien's model applied to a turbulent channel flow obeys:

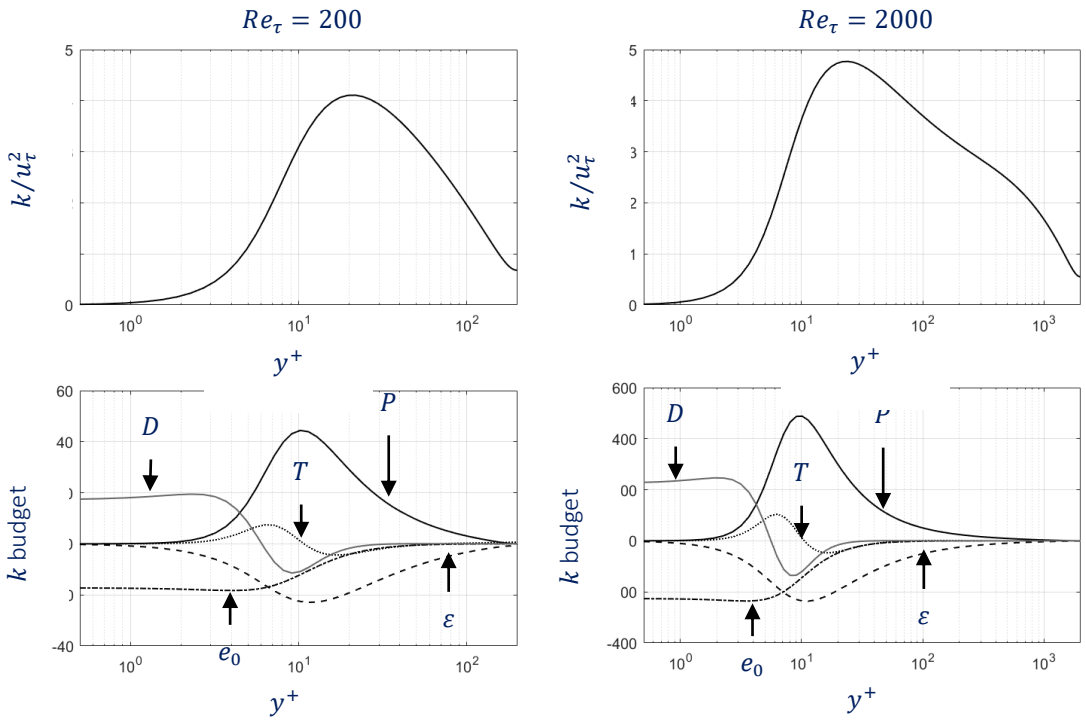

Figure 3: the behaviour of the k variable and its terms in Chien's $k-\varepsilon$ model.

$$0 = \underbrace{\tau_{ij}\frac{\partial U_i}{\partial x_j}}_{P} - \varepsilon - e_0 + \underbrace{\frac{\partial}{\partial x_j}\left(\frac{\nu_T}{\sigma_k}\frac{\partial k}{\partial x_j}\right)}_{T} + \underbrace{\nu\frac{\partial^2 k}{\partial x_j \partial x_j}}_{D}$$

The terms P, T and D denote respectively production, turbulent diffusion and viscous diffusion. The terms ε and e_0 are the dissipation terms. ε is active wherever its budget equation places it, whereas e_0 is only active next to walls and has the effect of suppressing k.

Inspection of Figure 3 (and Figure 1) reveals how closely k follows the real TKE and how closely its model budget follows the real TKE budget. The $k-\varepsilon$ model tries to replicate the positions of peak production and dissipation and the equilibrium nature of the flow away from the wall. The model also preserves the invariance of the budgets below $y^+ = 20$. The k budget of the Chien model differs from the true TKE budget because of the role of the function e_0 which modifies the shape of the dissipation term since it approaches the wall with a constant value.

The dissipation budget for the Chien model applied to the channel flow reads

$$0 = \underbrace{f_1 C_{\varepsilon 1}\frac{\varepsilon}{k}\tau_{ij}\frac{\partial U_i}{\partial x_j}}_{P} - \underbrace{f_2 C_{\varepsilon 1}\frac{\varepsilon^2}{k}}_{E} + e_1 + \underbrace{\frac{\partial}{\partial x_j}\left(\frac{\nu_T}{\sigma_\varepsilon}\frac{\partial \varepsilon}{\partial x_j}\right)}_{T} + \underbrace{\nu\frac{\partial^2 \varepsilon}{\partial x_j \partial x_j}}_{D}$$

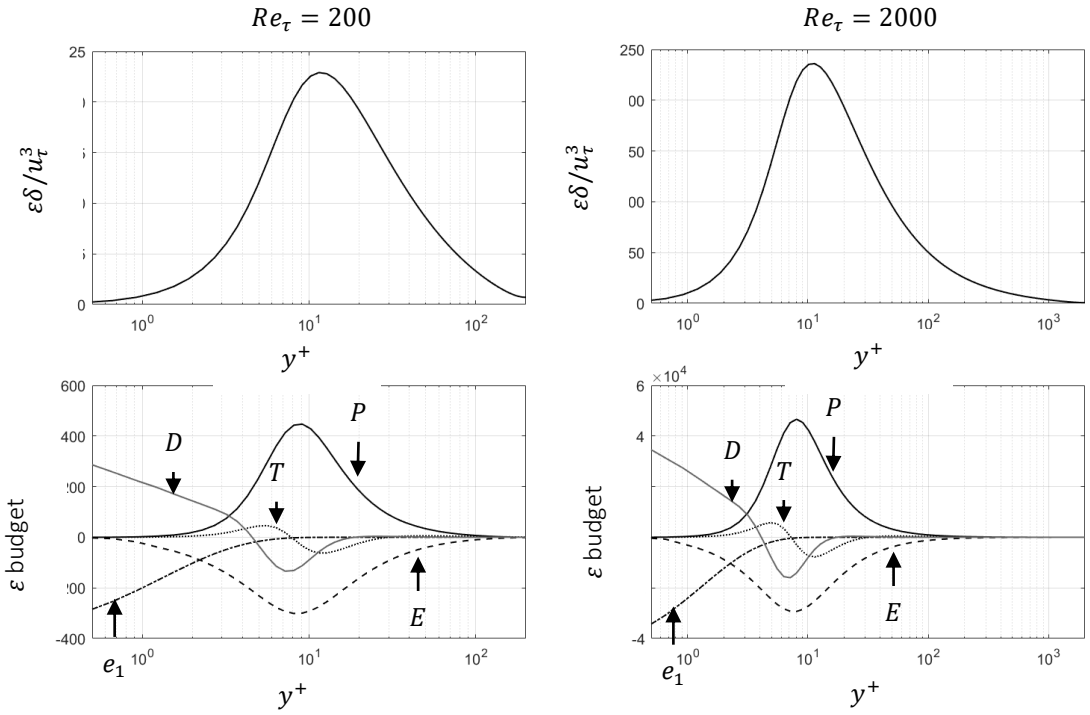

Figure 4: the behaviour of the ε variable and its terms in Chien's $k-\varepsilon$ model.

The variation of ε and of its budget terms is shown in Figure 4. ε has a peak at $y^+ \sim 10$ and decays to 0 towards the wall. This behaviour differs from the behaviour of the "true" dissipation rate inferred from DNS data (see Figure 1). The budget of ε is modelled on the k budget and therefore it follows a similar pattern: production and dissipation equilibrate each other above $y^+ \sim 10$ while near the wall the viscous diffusion is the only process balancing the low-Reynolds dissipation e_1. The turbulent diffusion T is only active in a narrow layer in proximity of the peak production.

2 The $k-\omega$ Model

The $k-\omega$ model is a popular alternative to the $k-\epsilon$ model. The original publication is

Wilcox, D. C., Rubesin, M. W. Progress in Turbulence Modeling for Complex Flow Fields Including Effects of Compressibility , April 1, 1980

The 1980 paper was preceded by a number of papers in the late 70s and was followed by an even larger number of follow-up papers documenting further refinements to the model. The most commonly used versions of the model are the one published in 1984 and Menter's SST (Shear Stress Transport) version, which blends the $k-\omega$ model with the $k-\epsilon$ model near shear layers.

The main motivation for the development of the $k-\omega$ is the ambiguity mentioned earlier with the ε equation. An additional shortcoming of the $k-\varepsilon$ model is that its

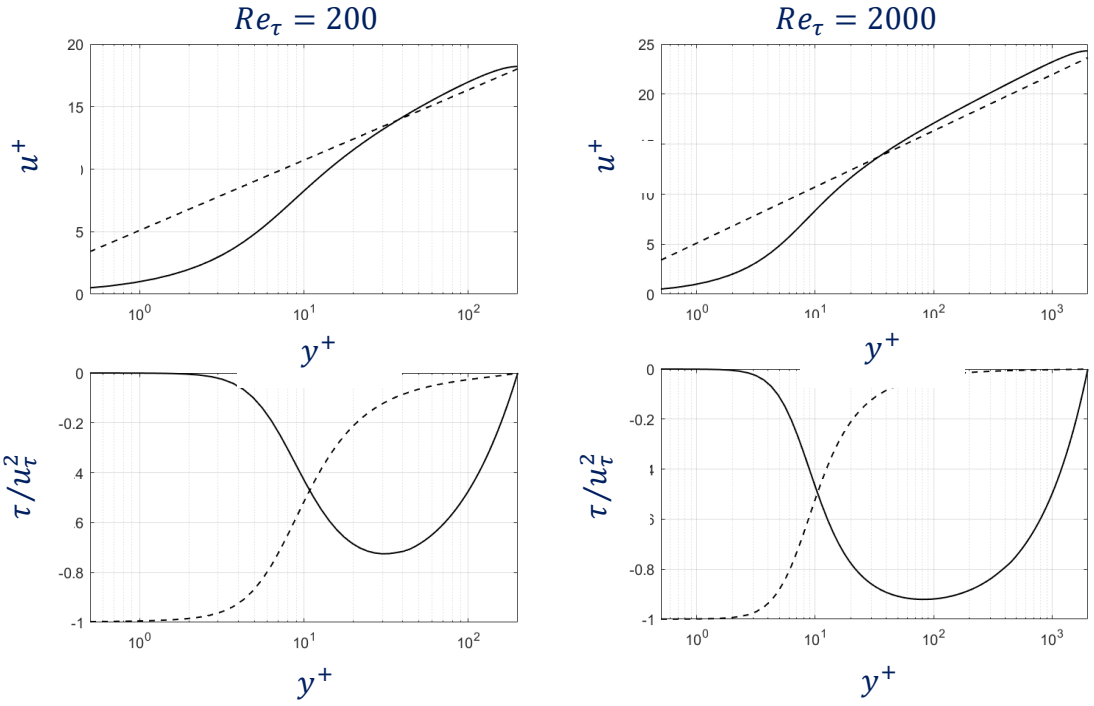

Figure 5: mean velocity profile and stress distributions from Wilcox' $k-\omega$ model for turbulent channel flow at Re_τ 200 and 2000**.**

Reynolds stress estimate is only appropriate if $\varepsilon \approx \tau_{ij}\frac{\partial U_i}{\partial x_j}$ (equilibrium flow). The $k-\omega$ model tries to resolve these issues by solving not a transport equation for ε but a (rather similar) transport equation for the specific dissipation rate

$$\omega = \varepsilon/k$$

The transport equation for ω does not have any ambition to represent a physical transport equation. Furthermore the relation between the k variable and the true TKE is weakened.

The eddy viscosity is evaluated as

$$\nu_T = k/\omega$$

The budget equation for the k variable is

$$\frac{\partial k}{\partial t} + U_j\frac{\partial k}{\partial x_j} = \tau_{ij}\frac{\partial U_i}{\partial x_j} - \beta^* k\omega + \frac{\partial}{\partial x_j}\left((\nu + \sigma^*\nu_T)\frac{\partial k}{\partial x_j}\right)$$

While the budget equation for the ω variable is

$$\frac{\partial \omega}{\partial t} + U_j\frac{\partial \omega}{\partial x_j} = \alpha\frac{\omega}{k}\tau_{ij}\frac{\partial U_i}{\partial x_j} - \beta\omega^2 + \frac{\partial}{\partial x_j}\left((\nu + \sigma\,\nu_T)\frac{\partial \omega}{\partial x_j}\right)$$

The closure coefficients are:

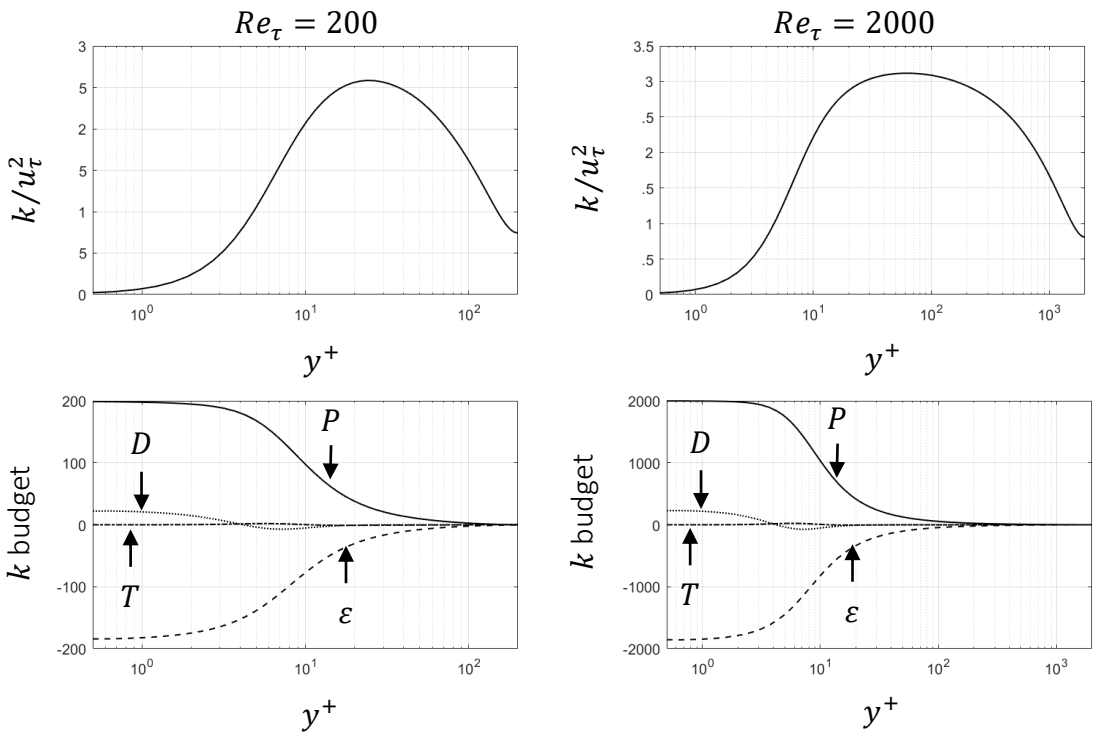

Figure 6: the behaviour of the k variable and its terms in Wilcox' $k-\omega$ model.

$$\alpha = 5/9, \qquad \beta = 3/40, \qquad \beta^* = 9/100, \qquad \sigma = \frac{1}{2}, \qquad \sigma^* = \frac{1}{2}$$

The appropriate boundary conditions for the $k-\omega$ model at a wall are

$$k \to 0$$

$$\omega \to \frac{6\nu}{\beta y^2}$$

The ω boundary condition needs to be enforced throughout the viscous layer to enforce the correct asymptotic behaviour near the wall.

2.1 Turbulent channel flow with the $k-\omega$ model

Figure 5 reports the results for turbulent channel flows at $Re_\tau = 200$ and 2000 from the $k-\omega$ model. The model manages to comply to the universal law of the wall reasonably well at low Reynolds number. More interesting are the graphs of the terms in the budget equation for k, shown in Figure 6. The budget equation, specialised for channel flow is reported below:

$$0 = \underbrace{\tau_{ij}\frac{\partial U_i}{\partial x_j}}_{P} - \underbrace{\beta^* k\omega}_{\varepsilon} + \underbrace{\frac{\partial}{\partial x_j}\left(\sigma^* \nu_T \frac{\partial k}{\partial x_j}\right)}_{T} + \underbrace{\nu\frac{\partial^2 k}{\partial x_j \partial x_j}}_{D}$$

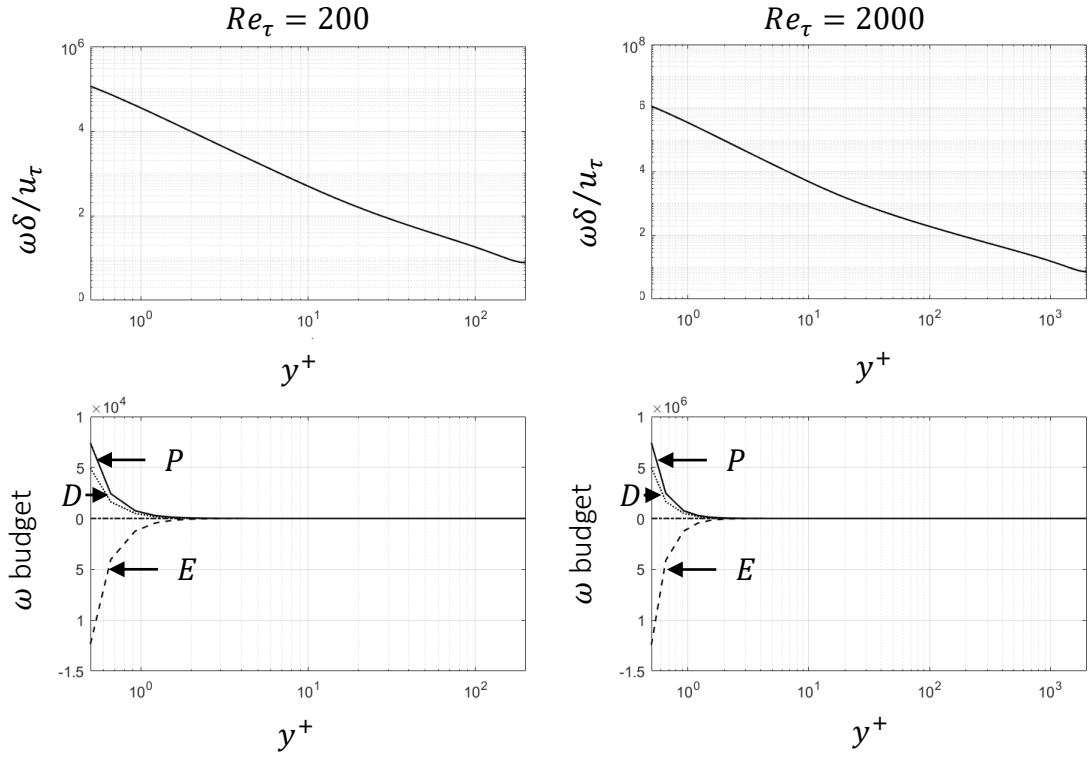

Figure 8: the behaviour of the ω variable and its terms in Wilcox' $k-\omega$ model.

We see that the budget of k in the $k-\omega$ looks very different from the TKE budget and the budget of k in the $k-\varepsilon$ model. In particular both the production and the dissipation of k reach finite limits at the wall and they essentially balance each other throughout the height of the channel. We also notice that the viscous diffusion makes a small contribution to replenishing the value of k near a wall, whereas the turbulent diffusion is essentially inactive in this test case.

The behaviour of the ω variable is shown in Figure 8. Here we see the effect of the boundary condition

$$\omega \to \frac{6\nu}{\beta y^2}$$

which forces ω to take large values next to the wall. The budget equation for ω in a turbulent channel flow is

$$0 = \underbrace{\alpha \frac{\omega}{k} \tau_{ij} \frac{\partial U_i}{\partial x_j}}_{P} - \underbrace{\beta \omega^2}_{E} + \underbrace{\frac{\partial}{\partial x_j}\left(\sigma \nu_T \frac{\partial \omega}{\partial x_j}\right)}_{T} + \underbrace{\nu \frac{\partial^2 \omega}{\partial x_j \partial x_j}}_{D}$$

Accordingly, the budget of ω is dominated by its rapid rise next to the wall. The dissipation E is balanced primarily by the production and to a comparable extent by the viscous diffusion near the wall.

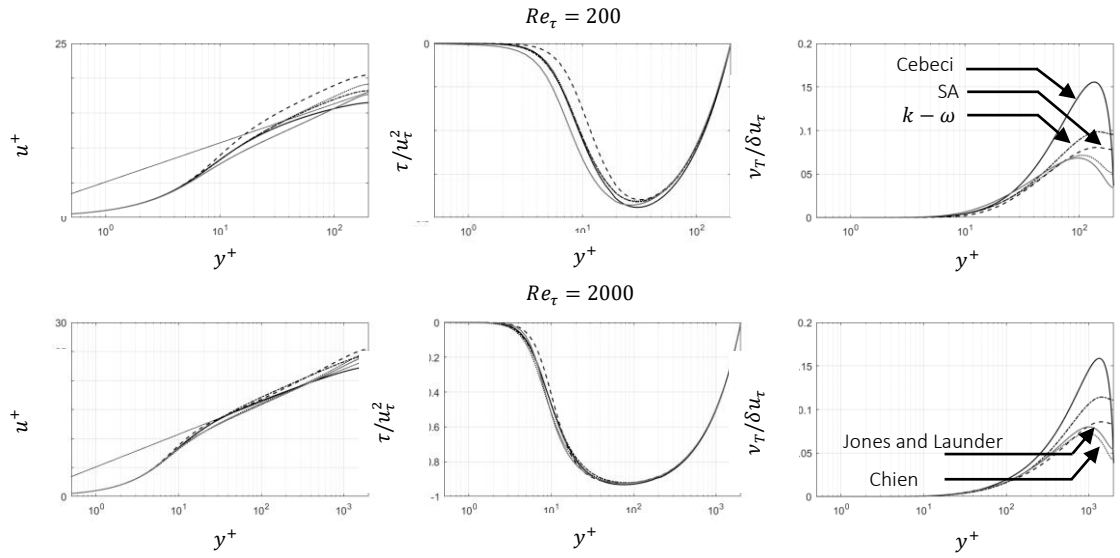

Figure 9: summary of channel flow results with the Cebeci, Spalart Allmaras, $k-\omega$, $k-\varepsilon$ (Chien and Jones/Launder) models

3 A summary of channel flow results

Figure 9 shows a summary of channel flow results obtained with the turbulence models presented so far.

It is clear that the agreement among the models for velocity profiles and Reynolds stresses improves at high Reynolds number, but it is also clear that the intermediate

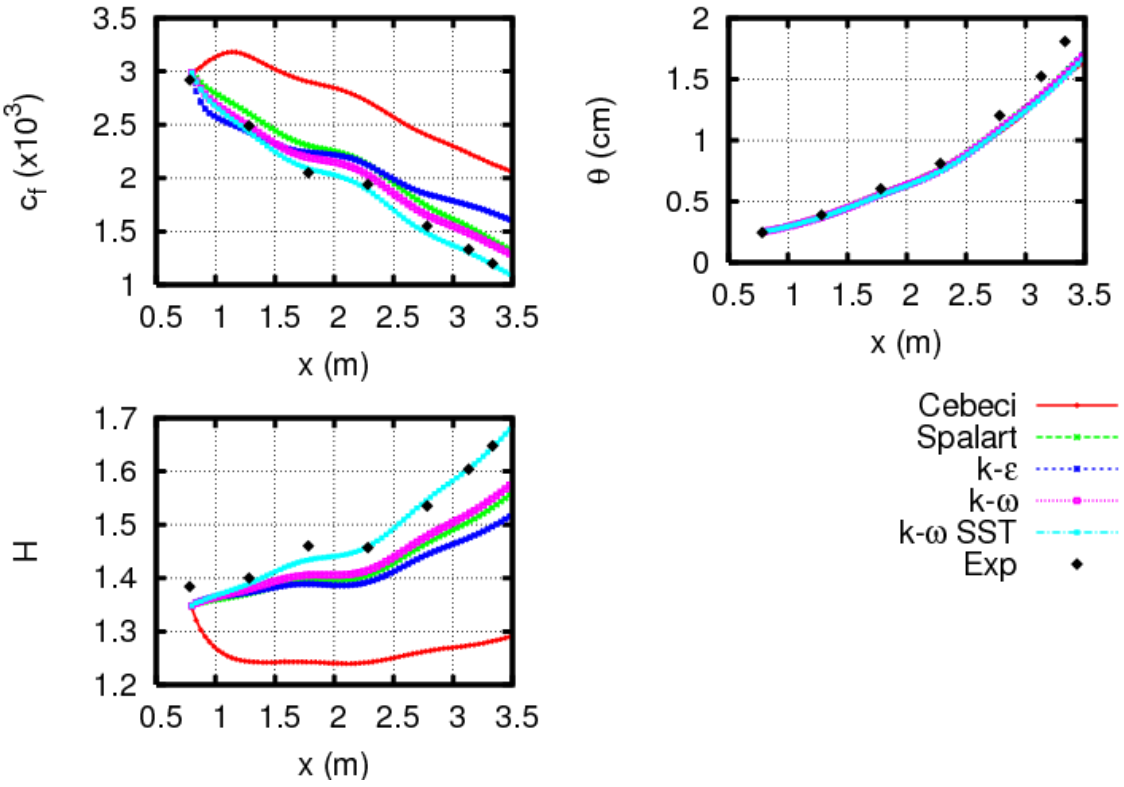

Figure 10: model predictions on adverse pressure gradient boundary layer

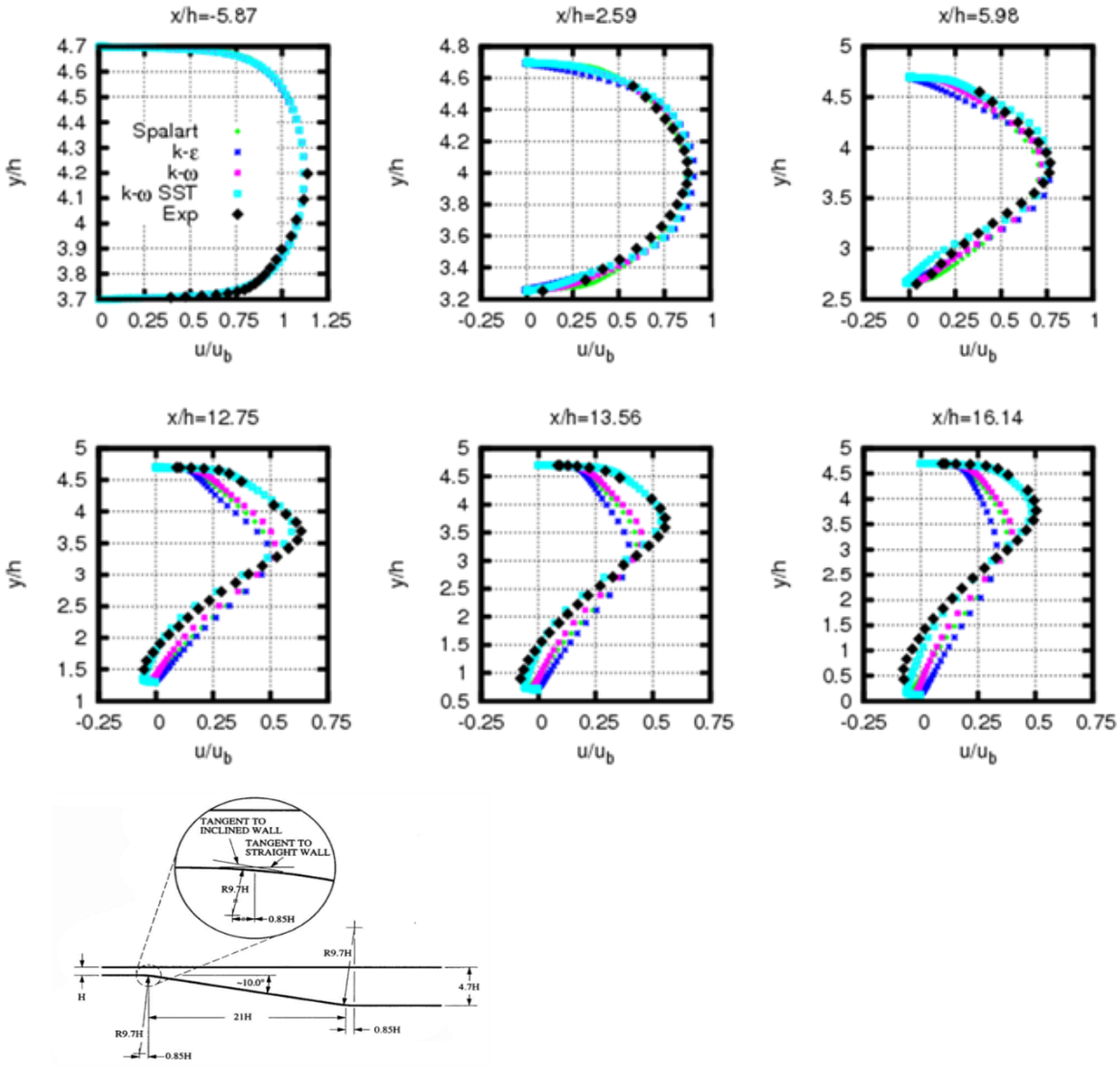

Figure 11: velocity profiles for the Eaton diffuser. The geometry of the diffuser is indicated in the diagram at the bottom.

variables of the models – such as the eddy viscosity -can be very different, despite the apparent agreement among the results regarding the mean flow.

4 Application to flows with pressure gradients

Figure 10 shows the results of computations with the models presented so far on a boundary layer with adverse pressure gradient. The models produce very different estimates for the friction coefficient and for the shape factor.

Figure 11 shows the same group of model applied to a diffuser. The diffuser is a typical example of a device where the flow is slowed down to increase pressure. The flow in a diffuser takes place against an adverse pressure gradient and is prone to separation. Turbulence models tend to perform poorly in presence of strong pressure gradients because an additional parameter enters the scaling laws for the Reynolds stress – the pressure gradient. As a consequence predictions with turbulence models generally disagree about the exact locations at which the flow separates and

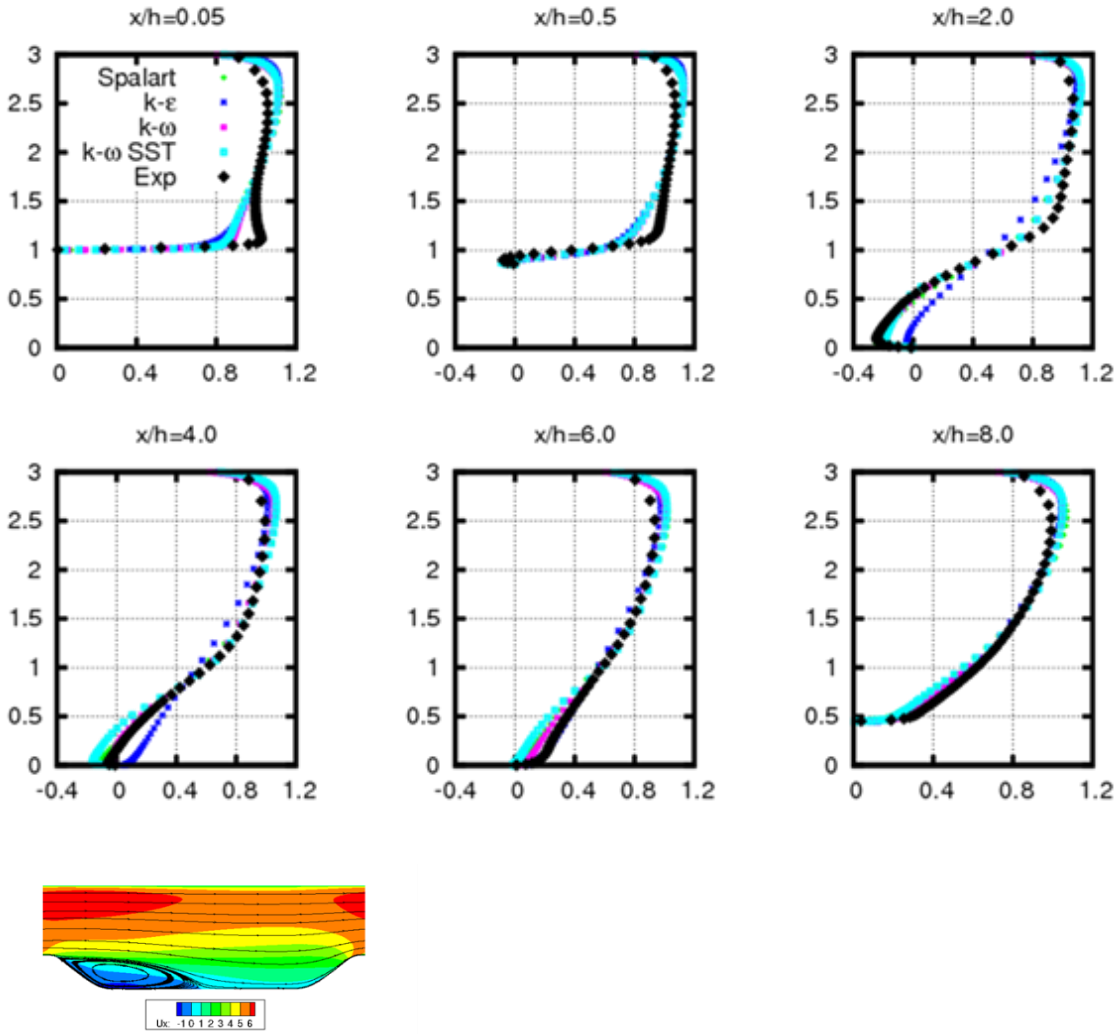

Figure 12: velocity profiles across periodic hills

reattaches. This phenomenon is clearly visible in the profiles in Figure 11, where separation is indicated by negative values of velocities.

A last set of results is shown in Figure 12. These results are velocity profiles in a channel with wavy walls. This flow is a model of flow over hilly terrain and is of interest in weather forecast for local weather patterns, the installation of wind turbines or the prediction of flow over urban landscapes.

Because of the slope of the walls, the flow separates on the down-wind side of each hill. We can see that all the models determine very different sizes and strengths of separation.

5 Linear eddy viscosity models: checklist

Boussinesq's hypothesis is the foundation of the linear eddy viscosity models. Boussinesq's hypothesis is based on an analogy between turbulent transport and molecular diffusion.

The main consequence of Boussinesq's hypothesis is the definition of an eddy viscosity which depends on a length scale (mixing length) and a velocity scale (turbulent velocity RMS).

We have encountered three classes of models based on the number of additional PDEs that need to be solved: 0 equations, 1 equation and 2 equations.

Applying Cebeci's model to the turbulent channel flow we have discovered that the log-law is implied by a mixing length that varies with distance from the wall. This implies that the eddies generating the Reynolds stress in a channel have dimensions limited by their distance from the wall.

We have examined in detail the behaviour of the Spalart Allmaras, $k-\varepsilon$ and $k-\omega$ models for channel flow and inspected the terms in the transport equations for the variables of these models.

We have discovered that even in a simple channel flow the turbulence models produce subtly different flow fields, which reflect considerable differences in intermediate variables such as eddy viscosities.

Application of turbulence models to diffusers, periodic hills and adverse pressure gradient boundary layers has shown that these models tend to perform best under mild pressure gradients and tend to disagree around separation and reattachment points.

6 Activities

The folder "Turbulence models" on Canvas contains Matlab functions to compute turbulent channel flows using the Cebeci, Spalart-Allmaras, Chien $k-\varepsilon$, Jones-Launders $k-\varepsilon$ and $k-\omega$ models. There are also scripts to produce plots similar to those in these notes and driver scripts to minimize input.

- The results from the Cebeci model in these notes showed a large value of the eddy viscosity at mid-channel compared to other models. How could you modify the input to the model to improve agreement with other models?
- The simulations in these notes were performed using grids with near-wall spacing of 0.2 wall units (see scripts with name starting with "run_"). How sensitive are the results to this parameter?
- Study the sensitivity of the predicted slope and intercept of the log-law to the closure constants of the Spalart-Allmaras, Chien $k-\varepsilon$ and $k-\omega$ model.